Repeated subconcussive head impacts compromise white matter integrity: A longitudinal DTI and NODDI study in collegiate football players

Sebastian D'Amario[1], Blaire Magee[1], Allen A. Champagne[1], Madison E. Wilson[1], Nicole S. Coverdale[1], Gabriel Ramírez-García[1,2], Douglas J Cook*[1,3]

*: Corresponding Author: dj.cook@queensu.ca

[1]Centre for Neuroscience Studies, Queen's University, Kingston, Canada

[2]Universidad Nacional Autonoma de Mexico, Mexico City, Mexico

[3]Department of Surgery, Queen's University, Kingston, Ontario, Canada

Abstract

Repetitive subconcussive impacts are a growing concern in contact sports due to their potential cumulative effects on brain structure, despite the absence of overt clinical symptoms. In this study, we investigated the effect of repeated subconcussive impact (RSCI) exposure on white matter (WM) microstructure in collegiate football players using advanced neuroimaging techniques. Twenty-two male athletes (ages 18-22) from the Queen's University Varsity Football Team were prospectively monitored over a single season. Participants were stratified into high-exposure (HE) and low-exposure (LE) groups based on impact frequency quantified with helmet-mounted accelerometers. MRI assessments, performed at pre-season, post-training camp, and post-season, included diffusion tensor imaging (DTI) metrics, including fractional anisotropy (FA) and mean diffusivity (MD), and neurite orientation dispersion and density imaging (NODDI) metrics, such as neurite density index (V_{in}), orientation dispersion index (ODI), and isotropic volume fraction (V_{iso}). Between-group comparisons revealed that HE athletes exhibited significantly lower FA and higher MD in the corticospinal tracts at pre-season, along with increased V_{iso} and reduced V_{in} and ODI in key association pathways compared to LE athletes. Longitudinal analyses demonstrated dynamic changes over the season, with significant alterations in diffusion metrics suggesting both acute injury responses and potential compensatory remodelling. These findings indicate that even in the absence of clinically diagnosed concussion, repetitive subconcussive impacts are associated with quantifiable changes in WM integrity. Our results underscore the need for improved monitoring and intervention strategies in contact sports to mitigate the risk of cumulative neural injury and to safeguard long-term brain health in athletes.

Introduction

Head injuries sustained during contact sport participation are increasingly recognized for their potential long-term effects on brain health.[1–3] While concussions have been extensively studied, increasing attention has focused on the effect of repetitive subconcussive impact (RSCI) exposure, as they occur much more frequently than concussion. In particular, high school and collegiate football players experience an average of 600 to 1400 impacts per season, depending on the level of play and position.[1,4] A subconcussive impact is defined as a head impact that does not produce observable clinical symptoms yet may still result in neurophysiological changes,[1,2] making them challenging to detect and address in real time. Nonetheless, neuroimaging studies have highlighted measurable changes in brain structure, particularly in WM microstructure. These changes may occur because the biomechanical forces underlying RSCIs (acceleration-deceleration impacts) may result in axonal shearing and neuronal disruption, initiating a cascade of neurochemical events that compromise WM integrity.[3,5]

Diffusion tensor imaging (DTI) has been instrumental in quantifying changes in WM integrity with metrics such as fractional anisotropy (FA) and mean diffusivity (MD).[6,7] FA measures how directionally restricted water movement is, while MD captures the overall amount of diffusion. Alterations in these metrics are associated with microstructural damage processes, including axonal injury and demyelination.[8] However, the findings in RSCI-related DTI studies have often been inconsistent, highlighting heterogeneity in WM changes.[9,10] For instance, FA and MD have both been shown to decrease[11–14] and increase[14,15] after RSCIs. Given these inconsistencies in DTI findings, researchers have increasingly turned to neurite orientation dispersion and density imaging (NODDI) for further quantification of advanced microstructural biomarkers. NODDI allows for a more nuanced characterization of microstructural properties by deriving advanced metrics, including neurite density (V_{in}), also known as intra-cellular volume

fraction,[16] which quantifies axonal and dendritic density; orientation dispersion index (ODI), which measures fiber orientation variability; and isotropic volume fraction (V_{iso}), which reflects the proportion of free water, providing complementary insights alongside DTI.[17] After exposure to RSCIs, ODI, V_{in}, and V_{iso} have been reported to increase,[11,12,18] possibly reflecting mechanisms such as neuroinflammation that increase free water.[19,20]

Combining DTI and NODDI may provide complementary insights into white matter microstructure. To our knowledge, only one prior longitudinal study has applied NODDI in this context, tracking year-to-year changes over four years in collegiate football and volleyball athletes.[18] This work revealed that non-concussed football players exhibited attenuated developmental trajectories, including smaller FA increases and reduced decreases in MD and ODI, compared to volleyball players, who displayed robust normative microstructural changes (e.g., pronounced FA increases and MD/ODI decreases).[18] While fewer studies have utilized NODDI, the metrics derived from this analysis may capture distinct aspects of microstructure that align with and expand upon DTI-based observations. Moreover, combining these modalities can provide a more comprehensive overview of the subtle and cumulative effects of SCI on WM integrity.[11]

In this study, our aim was to examine white matter microstructure in Canadian Varsity collegiate football players at three-time points over the course of a football season. By stratifying players into high- and low-exposure groups based on helmet accelerometer data, we investigated the cumulative effects of RSCIs on WM integrity and explored how these changes evolve over a football season, by comparing pre-season (PRE), post-training camp (PTC) and post-season (POST) time points. Additionally, the Sports Concussion Assessment Tool (SCAT3) was used to investigate the total number and severity of symptoms at all three time points.[21] We hypothesized that higher RSCI exposure would be associated with decreased FA and increased MD, as well as increased ODI, V_{in}, and V_{iso}, reflecting white matter

microstructural compromise. These changes are expected to be more pronounced in players with greater RSCI exposure compared to those with low exposure. These findings may contribute to a more comprehensive understanding of the neuropathophysiology of RSCIs to formulate future strategies for mitigating risks in contact sports.

Methods

Participants

Twenty-two male athletes from the Queen's University Varsity Football Team (ages 18–22; mean ± SD: 20 ± 1 years) in Kingston, Ontario, Canada participated in this study. Neuroimaging and neuropsychological assessments (SCAT3) were conducted at three time points: PRE, PTC (10 days following training camp), and POST (30 days following season's end). All athletes provided written informed consent, and the study was approved by the Queen's University Health Sciences Research Ethics Board. Participants all played in at least one previous season, and were excluded if they had pre-existing injuries, sustained injuries during the season that affected their ability to participate or had been diagnosed with a concussion within the past year or during the season.

Impact Monitoring

Subconcussive impact exposure was quantified using gForce Tracker (GFT) accelerometers (Artaflex Inc., Markham, Ontario, Canada). The devices were mounted inside each athlete's helmet using 3M Dual Lock™ Velcro, positioned at the left crown. Each accelerometer, capable of measuring linear acceleration and rotational velocity, was configured with a 15g threshold to exclude non-relevant movements (e.g. running, setting helmet down). During games and practices, on-site spotters flagged non-head impact events (e.g., dropped helmets) for subsequent removal. After a manual review of these instances, we calculated the

session average and cumulative impacts. Athletes were then stratified into high (HE; n = 11) and low (LE; = 11) exposure groups using a median average frequency of impacts per session[22] of 10.07 as the threshold.

MRI Acquisition

All MRI scans were conducted using a Siemens 3.0 T Magnetom Tim Trio system. T1-weighted structural images were acquired using an MP-RAGE sequence (TR = 1760 ms; TE = 2.2 ms; TI = 900 ms; matrix = 256 x 256; FOV = 256 mm^2; voxel size = 1 x 1 x 1 mm). We performed a diffusion-weighted fast spin-echo (TSE-DWI) sequence with the following parameters: TR = 7800 ms; TE = 95 ms; FOV = 256 mm^2; matrix = 128 x 128; 60 axial slices; voxel size = 1 x 1 x 1 mm, b-value = 1000 s/mm^2; and 30 gradient directions. Additionally, three non-diffusion-weighted (b = 0) images were acquired for normalization. Images were collected at the three time points under consistent conditions. Additionally, the SCAT3 symptom checklist was self-reported prior to each MRI. Higher scores on the SCAT3 indicate that the presence and severity of symptoms are more severe.

Neuroimaging Processing

Diffusion data were preprocessed using tools from FMRIB's Software Library (FSL).[23] Preprocessing steps included correction for susceptibility-induced distortions using the *topup* tool, correction for eddy currents and motion artifacts using *eddy*, and brain extraction with the *bet* tool. Diffusion tensors were calculated for each voxel using *dtifit* to produce maps of fractional FA and MD metrics for each subject. These maps were aligned to a standardized Montreal Neurological Institute (MNI152 2 mm) template using *FLIRT* and *FNIRT* for linear and non-linear registration, respectively.

NODDI was used to derive advanced microstructural metrics, V_{in}, ODI, and V_{iso}. Preprocessed diffusion-weighted images were used to fit the NODDI model parameters. A region-of-interest (ROI) file was generated for each subject, and a protocol incorporating b-values and b-vectors was constructed. The NODDI model (WatsonSHStickTortIsoV_B0) was fit to the data using a batch-fitting approach in MATLAB. Resulting V_{in}, ODI, and V_{iso} maps were aligned to a common space using non-FA Tract-Based Spatial Statistics (TBSS).

Tractography

Following preprocessing, probabilistic tractography was conducted to analyze WM tracts using BEDPOSTX, which models crossing fibres within each brain voxel. [24] Streamline density maps, generated using FSL's PROBTRACKX tool, quantified connectivity from the seed region to the target region for each tract. To ensure comparability across subjects, density maps were normalized by dividing each map by its waytotal using FSL's *fslmaths*. Waytotals represent the total number of streamlines reaching the target mask from the seed mask, accounting for inter-subject differences in scan quality or motion. In total, this was done for 12 bilateral tracts: Anterior Thalamic Radiation, Cingulate gyrus of Cingulum i.e. Cingulum (cingulate gyrus), Parahippocampal part of Cingulum i.e. Cingulum (hippocampus), Corticospinal Tract, Forceps Major, Forceps Minor, Inferior Fronto-occipital Fasciculus, Inferior Longitudinal Fasciculus, Posterior Thalamic Radiation, Superior Longitudinal Fasciculus, Superior Thalamic Radiation, Uncinate Fasciculus. Normalized tracts were registered to the MNI152 2mm standard space using *FLIRT* and *FNIRT* tools. Each tract was thresholded to eliminate low-probability streamlines, applying a consistent threshold of < 1% across subjects to ensure uniformity. Thresholded maps were then binarized to create masks for individual WM tracts. Tract-specific metric values were calculated by overlaying the binary masks onto standardized maps for each metric. The mean metric values for each subject and tract were extracted using FSL's *fslstats*

tool, enabling quantitative analysis of WM microstructure. Anatomical identification was done using the Human Xtract atlas.[25]

Statistical Analysis

Data distribution was assessed visually via histograms and Q-Q plots. To examine between-group differences (HE vs. LE) in diffusion metrics (FA, MD, V_{in}, ODI, and V_{iso}) at the three time points (PRE, PTC, POST) Mann-Whitney U tests were conducted for each WM tract. Glass rank-biserial correlation (r) was calculated as the effect size for these Mann-Whitney U tests.[26] These tests identified both the brain areas and the specific time points where significant group differences occurred. All statistical analyses was conducted in R (v4.2.2) and Prism (v10).

Changes in diffusion metrics across time points within each exposure group were analyzed using non-parametric one-way repeated-measures ANOVA (Friedman tests), with Kendall's W (W) reported as the effect size.[26] Kendall's W ranges from 0, indicating no relationship, to 1, indicating a perfect relationship. Further investigation with planned comparisons of within-group changes over time (such as PRE vs. POST) were conducted using Wilcoxon signed-rank tests, with rank-biserial correlation (r) also reported as the effect size.[26] All p-values were adjusted using Bonferroni corrections and are presented as Bonferroni-corrected values; in cases where the corrected p-values exceeded 1, they were truncated to 1. Statistical significance for all analyses was set at $p < 0.05$.

Linear mixed-effects models were used to analyze the SCAT3 scores. We specified our model with the dependent variables being the SCAT3 Symptom Score and Severity Score and included fixed effects of Group (HE vs. LE) and Time (PRE, PTC, POST), along with their interaction. Participant was incorporated as a random effect to account for inter-individual variability. This approach allowed us to examine the main effects of time and group, as well as their interaction, on the SCAT3 measures.

Results

Data collected from helmet accelerometers were used to examine the frequency of subconcussive impacts over the football season for each athlete. The 22 athletes enrolled in this study received a total of 7943 impacts across the football season, with the total impacts per subject ranging from 33 to 778 (Table 1). After separation into two groups based on the median impact frequency, overall, the LE group received 2512 impacts over the course of the season, compared to 5658 for HE, which is an average of 7.20 ± 0.177 impacts per session for LE versus 14.62 ± 0.381 impacts per session for HE.

Table 1. Average number of impacts overall and by session type

ID	Position	Group	Game	TC	Practice	Total	Sum for season
P-01	DB	LE	23.33	7.27	6.29	9.71	466
P-02	WR	LE	13.71	7.00	5.10	7.18	273
P-03	DB	LE	10.83	2.20	2.00	5.00	90
P-04	DL	LE	14.38	8.88	6.50	9.06	290
P-05	K	LE	3.14	2.00	1.80	2.54	33
P-06	WR	LE	19.00	11.00	4.33	9.00	216
P-07	WR	LE	11.57	5.13	3.11	4.90	206
P-08	LB	LE	7.33	4.71	2.26	3.58	129
P-09	DB	LE	15.71	6.00	5.83	7.64	298
P-10	DL	LE	10.00	8.00	8.00	8.29	232
P-11	LB	LE	14.86	10.78	5.20	9.00	279
P-12	OL	HE	25.50	12.91	10.19	13.39	509
P-13	WR	HE	26.88	8.57	6.58	11.10	433

P-14	DB	HE	40.13	9.60	6.36	12.93	595
P-15	LB	HE	20.13	13.44	4.61	10.43	422
P-16	DL	HE	26.00	21.73	12.26	16.91	778
P-17	OL	HE	12.00	14.55	15.55	15.00	495
P-18	WR	HE	26.20	26.78	9.95	17.00	561
P-19	DL	HE	36.67	19.11	19.29	21.23	552
P-20	DB	HE	27.86	3.75	4.78	11.17	268
P-21	DB	HE	33.00	7.40	4.00	11.18	369
P-22	RB	HE	45.25	9.67	4.75	17.45	506

DB, defensive back; DL, defensive line; K, kicker; LB, linebacker; OL, offensive line; RB, running back; TC, training camp; WR, wide receiver.

Based on the exposure groups described above, we examined white matter microstructural changes across three time points over a single football season. Using probabilistic tractography to reconstruct 12 tracts of interest, we assessed multiple diffusion metrics (FA, MD, V_{iso}, V_{in}, and ODI) for evidence of both between-group and within-group alterations. Figure 1 highlights the tracts with statistically significant changes in these metrics. All five metrics showed alterations in specific tracts between the HE and LE groups and within-group changes were documented for all metrics except ODI (Figure 1).

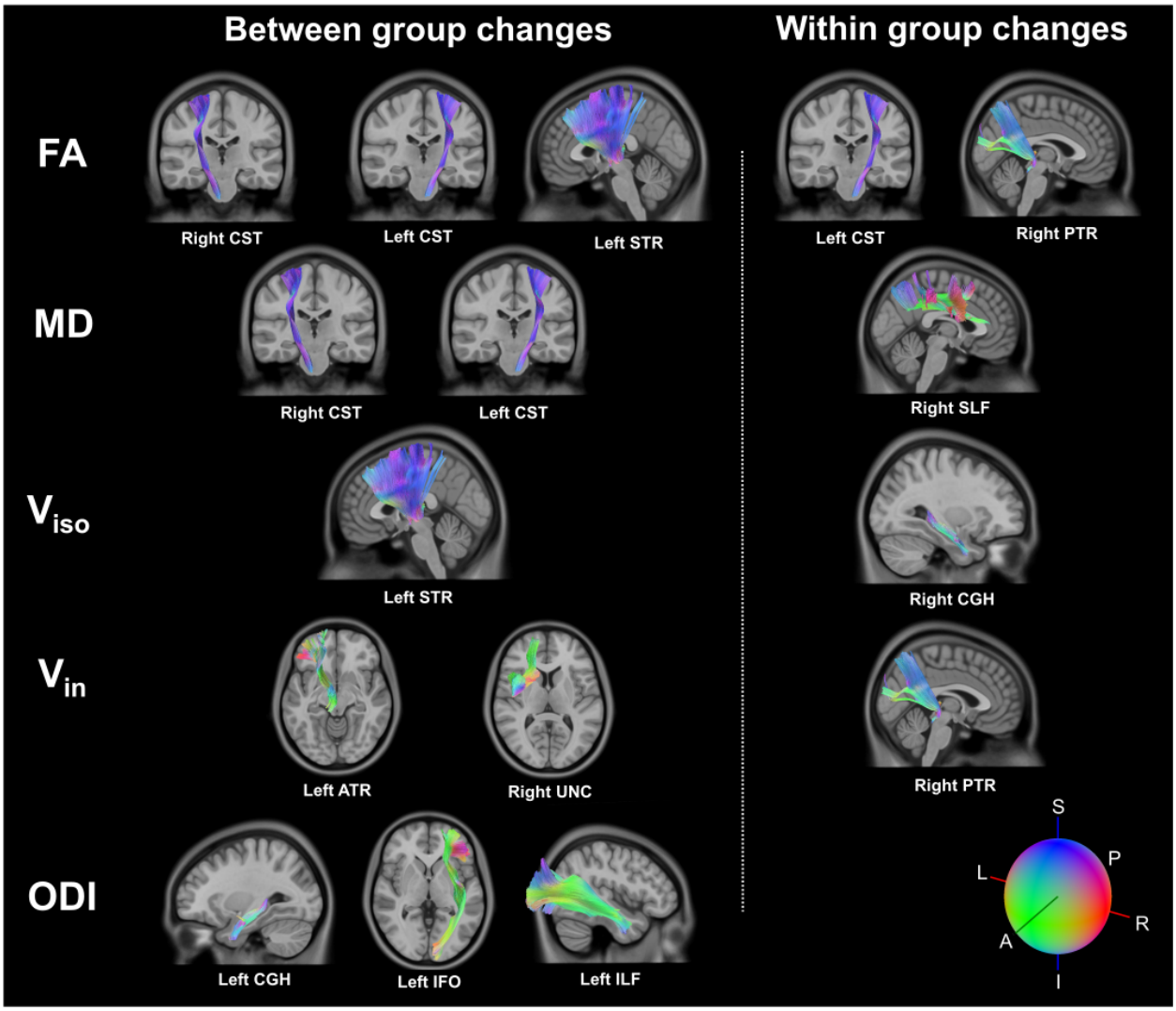

Figure 1. Probabilistic tractography outputs of WM tracts with altered metrics. Tract-based comparisons of diffusion measures showing both between-group (left column) and within-group (right column) effects on fractional anisotropy (FA), mean diffusivity (MD), isotropic volume fraction (V_{iso}), neurite density (V_{in}), and orientation dispersion index (ODI). Between groups, FA differences were identified in the left and right corticospinal tracts (CST) and the left superior thalamic radiation (STR); MD differences in the left and right CST; V_{iso} differences in the left STR; V_{in} differences in the left anterior thalamic radiation (ATR) and right uncinate fasciculus (UNC); and ODI differences in the left cingulum hippocampus (CGH), left inferior fronto-occipital fasciculus (IFO), and left inferior longitudinal fasciculus (ILF). Within groups, FA differences were found in the left CST and right posterior thalamic radiation (PTR); MD differences in the right superior longitudinal fasciculus (SLF); V_{iso} differences in the right cingulum hippocampus (CGH); and V_{in} differences in the right PTR. No significant within-group ODI changes survived Bonferroni correction. Coloured tract fibres are overlaid on a standard anatomical template for visualization.

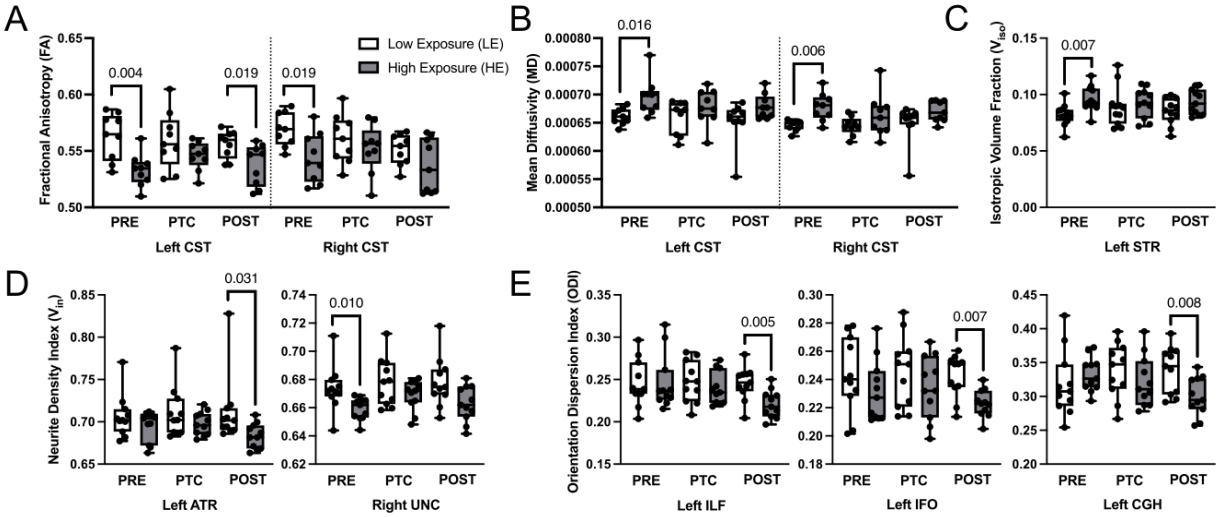

Figure 2. Between-group significant results of Mann-Whitney tests comparing Low Exposure (LE; white boxes) and High Exposure (HE; gray boxes) groups on diffusion MRI measures at three time points: PRE, PTC, and POST. All box-whisker plots show median values (center horizontal line), interquartile ranges (box boundaries), and the full data range (whiskers). The numerical values above the horizontal brackets denote the p-values for significant group differences. **A)** Fractional Anisotropy (FA) in the corticospinal tracts (CST). The left panel displays FA in the left CST decreased for the HE group at PRE and POST, and the right panel shows FA in the right CST decreased at PRE for HE. **(B)** Mean Diffusivity (MD) in the CST. Left CST (2B left) and right CST (2B right) show significant increases for HE at PRE. **C)** Isotropic Volume Fraction (V_{iso}) in the left superior thalamic radiation (STR) depicts an increase in V_{iso} at PRE for HE. **D)** Neurite Density Index (V_{in}) in association tracts. The left panel shows the left anterior thalamic radiation (ATR), with a significant decrease at POST for HE. The right panel shows the right uncinate fasciculus (UNC), where PRE indicates a significant decrease for HE. **E)** Orientation Dispersion Index (ODI) in key white matter pathways. The left inferior longitudinal fasciculus (ILF; 2E left), left inferior fronto-occipital fasciculus (IFO; 2E middle), and left cingulum (CGH; 2E right) are shown with significant decrease for the HE group compared to LE at POST.

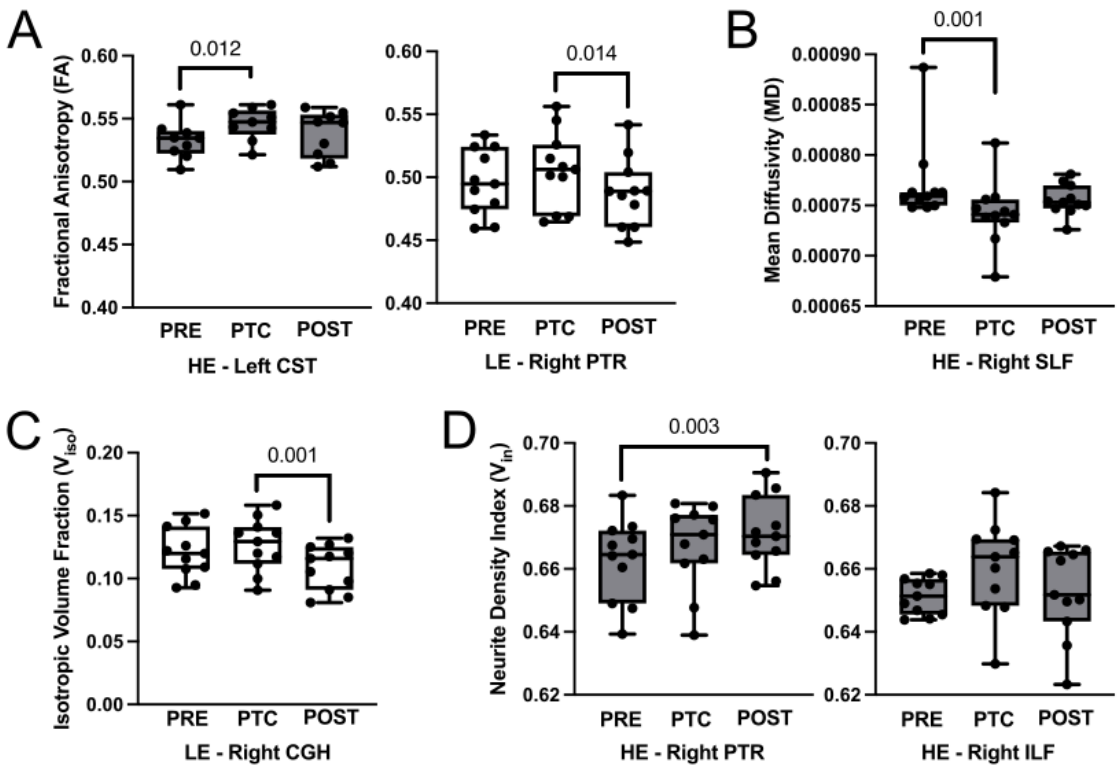

Figure 3. Within-group longitudinal changes in diffusion-based metrics for the High Exposure (HE; gray boxes) and Low Exposure (LE; white boxes) groups at PRE, PTC, and POST. All statistical comparisons were conducted using the Friedman test for repeated measures, with post-hoc Wilcoxon signed-rank tests. The p-values above each comparison indicate significant Wilcoxon results for specific time-point contrasts. Boxes represent group means (± standard deviation), with individual data points shown. **A)** Fractional Anisotropy (FA). Left: HE group in the left corticospinal tract (CST) exhibits a significant increase between PRE and PTC time points. Right: LE group in the right posterior thalamic radiation (PTR) shows a decrease from PTC and POST. **B)** Mean Diffusivity (MD) in the HE group for the right superior longitudinal fasciculus (SLF) showing a significant decrease from PRE to PTC. **C)** Isotropic Volume Fraction (V_{iso}) in the LE group for the right cingulum hippocampus (CGH) showing a significant decrease from PTC to POST. **D)** Neurite Density Index (V_{in}). Left: HE group in the right PTR, showing a significant increase from PRE to POST. Right: HE group in the right inferior longitudinal fasciculus (ILF). No significant within-group changes were detected following Bonferroni correction across the three time points.

Mann-Whitney U tests revealed that FA values in the corticospinal tracts were significantly different between the HE and LE groups at certain time points. In particular, the left corticospinal tract showed significantly lower FA in the HE group at PRE ($U = 9$, $p = 0.004$, $r = 0.778$; Fig 2A left) and at POST ($U = 14$, $p = 0.0188$, $r = 0.654$; Fig 2A left), both indicating large effect sizes. Similarly, the right corticospinal tract at PRE was also significantly lower for FA in

HE (U = 14, p = 0.0188, r = 0.654; Fig 2A right). Friedman tests examining changes over time indicated a significant difference in FA values for the left corticospinal tract in the HE group ($\chi^2(2, 11) = 9.455$, p = 0.0065, W = 0.524; Fig 3A left) and for the right posterior thalamic radiation in the LE group ($\chi^2(2, 11) = 9.455$, p = 0.0065, W = 0.43; Fig 3A right). Follow-up Wilcoxon signed-rank tests for the left corticospinal tract in the HE group demonstrated a significant increase between PRE and PTC (W = 41, p = 0.0351, r = 0.911; Fig 3A left), but no other significant differences were observed between time points. For the right posterior thalamic radiation in the LE group, the significant time effect was driven by a marked difference between PTC and POST (W = -54, p = 0.0411, r = 0.8182; Fig 3A right). No other FA differences were observed after accounting for multiple comparisons.

Significant between-group differences were found in MD for the corticospinal tracts. Specifically, the left corticospinal tract was significantly increased for HE at the PRE time point (U = 10, p = 0.0162, r = 0.753; Fig 2B left), and the right corticospinal tract was also significantly higher for HE at PRE (U = 7.5, p = 0.0063, r = 0.815; Fig 2B right), both indicating large effect sizes. No other tracts reached significance following correction for multiple comparisons. Longitudinal changes showed a significant time effect for the right superior longitudinal fasciculus in the HE exposure group ($\chi^2(2, 11) = 12.18$, p = 0.0022, W = 0.553; Fig 3B), indicating a large effect size. Follow-up tests indicated this effect was driven by a significant decrease between PRE and PTC (W = -66, p = 0.003, r = 0.4394; Fig 3B). All other time comparisons and tracts showed no significant changes after adjustment for multiple comparisons.

The NODDI metric V_{iso} was significantly lower in the left superior thalamic radiation at the PRE time point for the LE group compared to HE (U = 16, p = 0.0072, r = 0.736; Fig 2C). Across the LE group, we found a significant difference in the right cingulum hippocampus ($\chi^2(2, 11) = 8.91$, p = 0.022; Fig 3C). The effect size, measured by Kendall's W, was moderate (W =

0.405). Follow-up Wilcoxon signed-rank tests revealed the finding was driven by the difference between PTC and POST in the LE group (W = -66, p = 0.001, r = -1; Fig 3C), with a perfect negative effect size demonstrating that all participants at POST were lower than they were at PTC. There was no significant difference between other time points in the analysis.

Mann-Whitney U tests revealed that the V_{in} metric was significantly lower in the HE group compared to the LE group for the left anterior thalamic radiation at the POST time point (U = 22, p = 0.031, r = 0.636; Fig 2D left). Additionally, the right uncinate fasciculus showed a significant decrease in the HE group compared to the LE group at the PRE time point (U = 17, p = 0.0096, r = 0.719; Fig 2D right). Longitudinally, we found a significant difference in the right posterior thalamic radiation scores across time points for the HE exposure group ($\chi^2(2, 11) = 9.46$, p = 0.0065, W = 0.43; Fig 3D left), indicating a large effect size. Follow-up tests indicated this result was driven by a significant increase between PRE and POST (W = 66, p = 0.003), with a perfect effect size (r = 1) meaning all individuals showed the same increased direction of change from PRE to POST (Fig 3D left). No significant differences were observed between other time points in the analysis. The right inferior longitudinal fasciculus in the HE group also indicated a significant overall difference across time points ($\chi^2(2, 11) = 7.818$, p = 0.0374, W = 0.355; Fig 3D right). After Bonferroni correction, none of the follow-up Wilcoxon signed-rank tests remained significant (PTC vs PRE: W = 46, p = 0.042, adjusted p = 0.126, r = 0.697; POST vs PRE: W = 8, p = 0.7646, adjusted p = 1, r = 0.1212; POST vs PTC: W = -42, p = 0.0674, adjusted p = 0.2022, r = -0.6364; Fig 3D right). This discrepancy suggests that while the global Friedman test showed changes over time, the specific pairwise comparisons were not robust enough to reach significance once the more stringent Bonferroni correction was applied.

The ODI metric was significantly lower in the HE group compared to the LE group at the POST time point for several tracts. Specifically, the left inferior longitudinal fasciculus (U = 19, p = 0.0052, r = 0.686; Fig 2E left), the left inferior fronto-occipital fasciculus (U = 20, p = 0.0066, r

= 0.6694; Fig 2E middle) and the left cingulum (hippocampus) demonstrated a significant reduction (U = 21, p = 0.0083, r = 0.6529; Fig 2E right). All findings remained significant after Bonferroni correction and demonstrated large effect sizes. A Friedman test examining longitudinal changes in ODI found no significant differences observed across the tracts or time points.

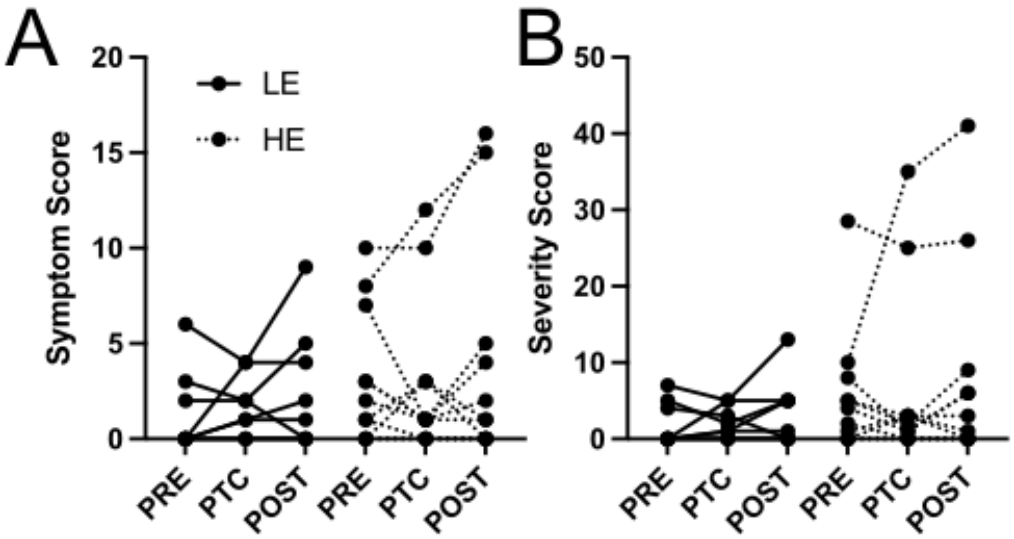

Figure 4. SCAT3. Each line represents the change in a participant's score over the season. **A.** total symptom scores and **B.** severity scores are displayed across PRE, PTC, and POST time points. Linear mixed-effects models suggest no significant differences and that symptom reports remained stable.

We then examined the Symptom and Severity Scores, obtained from SCAT3, and compared it across PRE, PTC and POST. In the Symptom Score model, scores at PRE were lower than POST (mean difference = -0.82, p = 0.28) and at PTC were lower than POST (mean difference = -1.09, p = 0.15). Similarly, in the Severity Score model, scores at PRE were lower than POST (mean difference = -2.59, p = 0.17) and at PTC were lower than POST (mean difference = -1.73, p = 0.36). However, none of these timepoint differences reached statistical significance. In addition, while the LE group tended to have lower scores than the HE group (Symptom Score: mean difference = -1.38, p = 0.46; Severity Score: mean difference = -4.74 p

= 0.26), the interaction effects did not indicate significant differences in score trajectories between groups. Specifically, for the Symptom Score model, the LE versus HE differences were -0.43 at PRE ($p > 0.70$) and 0.22 at PTC ($p > 0.70$), and for the Severity Score model, they were 0.97 at PRE ($p > 0.70$) and 0.23 at PTC ($p > 0.70$). In summary, the models suggest no differences in the trajectories of either Symptom or Severity Scores between the HE and LE groups over the measured timepoints (PRE, PTC, POST). Despite some numerical trends, the changes in scores over time do not differ reliably between groups based on the current data.

Discussion

RSCIs have increasingly been implicated in subtle yet cumulative alterations in WM microstructure, even in the absence of clinically diagnosed concussion.[2,14] In this study, HE athletes exhibited significantly lower FA and higher MD in the corticospinal tracts at the PRE time point. HE athletes also had increased V_{iso} and reduced V_{in} and ODI at various timepoints in key association pathways, such as the anterior thalamic radiation and uncinate fasciculus, compared to LE. These findings support our hypothesis that greater RSCI exposure would be associated with alterations in microstructure. Notably, significant group differences were already apparent at the PRE time point (when athletes had paused from contact sports for several months), suggesting cumulative WM changes may be attributable to prior seasons of play. While seasonal changes in microstructure were modest across exposure groups compared to the marked baseline differences observed at PRE, HE athletes demonstrated unique longitudinal changes in diffusion metrics over the season. Specifically, HE athletes exhibited dynamic alterations in diffusion metrics over the season, characterized by initial deviations from PRE values at PTC, followed by a partial return toward baseline at POST. This pattern was most pronounced in the corticospinal tract and superior longitudinal fasciculus, where metrics shifted acutely at PTC but trended back toward pre-season levels by POST. These findings suggest that even in the context of significant baseline differences, HE athletes displayed

distinct longitudinal trajectories reflecting transient microstructural changes during the season, rather than sustained progressive declines or elevations.

When comparing groups at each seasonal time point (PRE, PTC, POST), the HE group displayed consistently larger differences in diffusion metrics relative to the LE group, including both DTI (FA, MD) and NODDI (V_{in}, V_{iso}, ODI) measures. At PRE, HE athletes exhibited lower FA and higher MD in bilateral corticospinal tracts compared to LE athletes. This suggests unresolved axonal disruption from prior seasons of football,[13] and is consistent with earlier research indicating that WM damage in contact-sport athletes can persist well beyond the season's end.[27–29] At POST, these differences remained in the left corticospinal tract, supporting our hypothesis and prior research linking higher impact frequency to greater WM disruptions.[30,31] The corticospinal tracts, compact and unidirectional, are essential for voluntary motor control.[32] Their organized structure may offer some protection compared to more diffusely oriented fibres, yet repeated strain in biomechanically vulnerable regions, such as those impacted during tackles or collisions, can still lead to cumulative microstructural disruption. This underscores the importance of assessing both tract-specific features and biomechanical context when evaluating RSCI-related damage, the latter of which should be explored in future work.

NODDI results further underscored group disparities. In the HE group, V_{in} was significantly reduced in the left anterior thalamic radiation at POST and in the right uncinate fasciculus at PRE, suggesting diminished axonal or dendritic architecture in heavily exposed players, compared to LE. This reduction in V_{in} is consistent with previous reports in mTBI, where it was found to be 5-9% lower in injured brains.[33] Similarly, the lower V_{in} in the HE group found in this study mirrors the Palacios et al. (2020) finding of progressive neurite density reductions. We find this alongside a general trend of increased V_{iso}, which reflects higher free-water content or extracellular space: in line with previous observations.[11,12] In our study, the higher V_{iso} observed in the HE group aligns with the idea of increased extracellular space following

repetitive head impacts. HE athletes demonstrated reduced ODI at POST in specific white matter tracts (including the left inferior longitudinal fasciculus, inferior fronto-occipital fasciculus, and cingulum hippocampus) compared to LE athletes. ODI reflects the dispersion of axon orientations within a voxel; reduced ODI indicates microstructural simplification, a loss of axonal complexity that may stem from mechanisms such as axonal injury, reduced dendritic branching, or glial scarring.[34] These notable microstructural changes observed through NODDI continue to support its sensitivity and utility alongside DTI in RSCI research.

Longitudinal analyses revealed fluctuations in FA for both the LE and HE groups. The HE group had significantly higher FA at PTC compared to PRE, but interestingly, the LE group showed significant decreases in FA from PTC to POST in the right posterior thalamic radiation, implying that reduced impact frequency does not entirely protect athletes from microstructural disruption.[10,35,36] In contrast, changes in the HE group for MD were only evident with short-term decreases in MD during PTC that could reflect transient axonal swelling or edema/possibly reflecting acute axonal swelling or cytotoxic edema.[13] The bidirectional shifts (both increases and decreases) in diffusion metrics over a season align with previous work suggesting that repeated head impacts trigger cycles of axonal injury, partial recovery, and ongoing susceptibility to insult.[13,14] Such cyclical processes may help explain the inconsistencies seen across different studies, as each may be capturing different phases of axonal pathology or repair.

Over the season, the LE group showed a significant decrease in V_{iso} in the right cingulum hippocampus from PTC to POST, suggesting reduced extracellular or free-water space, potentially reflecting the resolution of acute edema or early signs of atrophy. This observation aligns with Palacios et al. (2020), who documented longitudinal V_{iso} decreases in posterior WM tracts following an early increase post-injury. Conversely, the HE group exhibited a robust increase in V_{in} within the right posterior thalamic radiation between PRE and POST, hinting at a

compensatory or reorganizational response within the WM microstructure over the season. Although Palacios et al. (2020) generally reported progressive V_{in} reductions, they also noted instances of temporary increases that could represent reactive plasticity. This interpretation is further supported by findings from Goubran et al. (2023), who demonstrated an attenuated increase in V_{in} in football players (particularly those with concussive histories) compared to low-contact athletes. These works suggest that RSCIs in high-exposure athletes trigger a dual process of injury and repair, with certain tracts exhibiting evidence of compensatory remodelling over time. Together, the findings highlight that different facets of microstructure (e.g., fibre density vs. extracellular space) may follow distinct trajectories in response to repetitive head impacts.

Our longitudinal design revealed that ODI declines in HE athletes became evident only after sustained in-season activity, contrasting with cross-sectional studies reporting elevated ODI in MMA fighters[11] and football players[12] at single timepoints. Minimal work has been done on the long-term changes of RSCIs associated with NODDI metrics. However, Goubran et al. (2023) observed progressive ODI declines in control volleyball players over four years, attributing this to healthy neurodevelopmental processes (e.g., myelination, synaptic pruning), where simplification reflects streamlined axonal organization.[18] Conversely, their RSCI-exposed football cohort exhibited no ODI decline over the same period, suggesting neurostructural disruption (e.g., suppressed pruning due to repetitive head impacts).[18] RSCI exposure initiates inflammatory cascades that are suggested to disrupt synaptic pruning, which is a critical process for refining and optimizing neural connections.[37] This impairment could transiently influence ODI by sustaining tissue heterogeneity, as disrupted pruning prevents the connectivity streamlining observed in healthy populations.[18] Our results extend these observations: POST ODI reductions in HE athletes may reflect an acute phase of microstructural simplification, consistent with WM adaptation driven by RSCI exposure,[13] distinct from Goubran's volleyball

cohort's adaptive declines. Further, prolonged exposure (e.g., four years in Goubran's football cohort) could impair the brain's capacity for adaptive simplification, instead stabilizing ODI due to pathological mechanisms (e.g., chronic inflammation) which masks normative ODI trajectories.[38] Thus, while cross-sectional studies highlight ODI elevations as markers of inflammation, our between-group longitudinal data emphasize non-linear, phase-specific dynamics. Reductions in diffusion metrics, including ODI, are mechanistically ambiguous: they may signify either adaptive plasticity (long-term, low-impact contexts) or early microstructural compromise (short-term, high-impact contexts), depending on sport-specific demands and exposure duration. Collectively, these findings highlight the importance of interpreting ODI changes within a multimodal framework that includes complementary diffusion metrics, as a comprehensive approach can better reveal the holistic underlying microstructural changes associated with RSCIs.

Despite these insights, several limitations warrant mention. First, the small sample size (n = 22) limited statistical power and may have contributed to non-significant trends. Larger cohorts could enable parametric analyses and more robust assessments of interaction effects. Second, the absence of a non-contact control group makes it difficult to distinguish changes related to head impacts from general athletic factors.[39,40] Although comparing HE and LE athletes supports a dose-response relationship, a control group would clarify how physical exertion alone influences DTI and NODDI measures. Despite three time points being evaluated, a multi-season longitudinal approach in the same individuals would help determine whether RSCI-related injuries accumulate or partially heal over extended off-season intervals. Incorporating immediate pre- and post-game MRI scans could provide a closer look at the hyperacute phase of axonal swelling, while follow-up imaging several months after the season could clarify whether the microstructure normalizes or remains altered. Building on Goubran et al. (2023), who found no significant results using the global SCAT score, we examined SCAT

sub-scores to assess symptom and severity changes. Despite white matter alterations, we found no significant differences in sub-scores, reinforcing the concern that SCAT3 may lack the sensitivity to detect subtle, cumulative effects of RSCIs over time. Thus, integrating DTI/NODDI data with more comprehensive behavioural and clinical scales would help to elucidate how subclinical WM changes translate into long-term neurological outcomes.[31,41]

In conclusion, our results indicate that high frequency subconcussive impacts can produce quantifiable and possibly enduring alterations to WM microstructure, which may accumulate silently across multiple seasons of play. Reduced FA, V_{in} and ODI with increased MD and V_{iso} collectively point to subtle but meaningful axonal disruption in heavily exposed athletes. Together, the bidirectional and region-specific trajectories of DTI/NODDI metrics suggest that repetitive head impacts induce a dynamic interplay between acute axonal injury and compensatory remodeling, with the balance shifting depending on impact dose, tract vulnerability, and temporal proximity to exposure. This pattern implies that factors such as player position, style of play, and starting status could potentially result in similar impact profiles across seasons for a player. While the precise timeline and clinical implications remain uncertain, these findings highlight the need for continued efforts to mitigate repetitive head impacts in contact sports, whether through refined tackling practices, equipment improvements, or strategic rule changes. By characterizing how RSCIs influences brain structure and exploring how that structure recovers or degrades over time, researchers and clinicians can better delineate risks, identify thresholds for safe participation, and develop targeted interventions to preserve athlete brain health.

References

1. Bailes, J. E., Petraglia, A. L., Omalu, B. I., Nauman, E. & Talavage, T. Role of subconcussion in repetitive mild traumatic brain injury. *J. Neurosurg.* **119**, 1235–1245 (2013).
2. Mainwaring, L., Ferdinand Pennock, K. M., Mylabathula, S. & Alavie, B. Z. Subconcussive head impacts in sport: A systematic review of the evidence. *Int. J. Psychophysiol.* **132**, 39–54 (2018).
3. Blennow, K., Hardy, J. & Zetterberg, H. The neuropathology and neurobiology of traumatic brain injury. *Neuron* **76**, 886–899 (2012).
4. Broglio, S. P. *et al.* Head Impacts During High School Football: A Biomechanical Assessment. *J. Athl. Train.* **44**, 342–349 (2009).
5. MacFarlane, M. P. & Glenn, T. C. Neurochemical cascade of concussion. *Brain Inj.* **29**, 139–153 (2015).
6. Alexander, A. L., Lee, J. E., Lazar, M. & Field, A. S. Diffusion tensor imaging of the brain. *Neurother. J. Am. Soc. Exp. Neurother.* **4**, 316–329 (2007).
7. Tournier, J.-D., Mori, S. & Leemans, A. Diffusion tensor imaging and beyond. *Magn. Reson. Med.* **65**, 1532–1556 (2011).
8. Assaf, Y. & Pasternak, O. Diffusion tensor imaging (DTI)-based white matter mapping in brain research: a review. *J. Mol. Neurosci. MN* **34**, 51–61 (2008).
9. Chun, I. Y. *et al.* DTI Detection of Longitudinal WM Abnormalities Due to Accumulated Head Impacts. *Dev. Neuropsychol.* **40**, 92–97 (2015).
10. McAllister, T. W. *et al.* Effect of head impacts on diffusivity measures in a cohort of collegiate contact sport athletes. *Neurology* **82**, 63–69 (2014).
11. Mayer, A. R. *et al.* A prospective microstructure imaging study in mixed-martial artists using geometric measures and diffusion tensor imaging:

methods and findings. *Brain Imaging Behav.* **11**, 698–711 (2017).

12. Caron, B. *et al.* Advanced mapping of the human white matter microstructure better separates elite sports participation. Preprint at https://doi.org/10.31234/osf.io/dxaqp (2020).
13. Bazarian, J. J. *et al.* Persistent, Long-term Cerebral White Matter Changes after Sports-Related Repetitive Head Impacts. *PLOS ONE* **9**, e94734 (2014).
14. Bazarian, J. J., Zhu, T., Blyth, B., Borrino, A. & Zhong, J. Subject-specific changes in brain white matter on diffusion tensor imaging after sports-related concussion. *Magn. Reson. Imaging* **30**, 171–180 (2012).
15. Hellewell, S. C., Nguyen, V. P. B., Jayasena, R. N., Welton, T. & Grieve, S. M. Characteristic patterns of white matter tract injury in sport-related concussion: An image based meta-analysis. *NeuroImage Clin.* **26**, 102253 (2020).
16. Muller, J. *et al.* Hybrid diffusion imaging reveals altered white matter tract integrity and associations with symptoms and cognitive dysfunction in chronic traumatic brain injury. *NeuroImage Clin.* **30**, 102681 (2021).
17. Zhang, H., Schneider, T., Wheeler-Kingshott, C. A. & Alexander, D. C. NODDI: Practical in vivo neurite orientation dispersion and density imaging of the human brain. *NeuroImage* **61**, 1000–1016 (2012).
18. Goubran, M. *et al.* Microstructural Alterations in Tract Development in College Football and Volleyball Players: A Longitudinal Diffusion MRI Study. *Neurology* **101**, (2023).
19. Fick, R. H. J. *et al.* Comparison of biomarkers in transgenic alzheimer rats using multi-shell diffusion MRI. in *Computational Diffusion MRI - MICCAI Workshop* 187–199 (Springer Heidelberg, 2017). doi:10.1007/978-3-319-54130-3_16.
20. Suzuki, H. *et al.* Abnormal brain white matter microstructure is associated with

both pre-hypertension and hypertension. *PloS One* **12**, e0187600 (2017).

21. Guskiewicz, K. M. *et al.* Evidence-based approach to revising the SCAT2: introducing the SCAT3. (2013) doi:10.1136/bjsports-2013-092225.
22. Champagne, A. A., Coverdale, N. S., Germuska, M., Bhogal, A. A. & Cook, D. J. Changes in volumetric and metabolic parameters relate to differences in exposure to sub-concussive head impacts. *J. Cereb. Blood Flow Metab. Off. J. Int. Soc. Cereb. Blood Flow Metab.* **40**, 1453–1467 (2020).
23. Jenkinson, M., Beckmann, C. F., Behrens, T. E. J., Woolrich, M. W. & Smith, S. M. FSL. *NeuroImage* **62**, 782–790 (2012).
24. Behrens, T. E. J., Berg, H. J., Jbabdi, S., Rushworth, M. F. S. & Woolrich, M. W. Probabilistic diffusion tractography with multiple fibre orientations: What can we gain? *NeuroImage* **34**, 144–155 (2007).
25. Warrington, S. *et al.* XTRACT - Standardised protocols for automated tractography in the human and macaque brain. *NeuroImage* **217**, 116923 (2020).
26. Tomczak, M. & Tomczak, E. The need to report effect size estimates revisited. An overview of some recommended measures of effect size. **1**, (2014).
27. Henry, L. C. *et al.* Acute and chronic changes in diffusivity measures after sports concussion. *J. Neurotrauma* **28**, 2049–2059 (2011).
28. Lancaster, M. A. *et al.* Chronic differences in white matter integrity following sport-related concussion as measured by diffusion MRI: 6-Month follow-up. *Hum. Brain Mapp.* **39**, 4276–4289 (2018).
29. Stamm, J. M. *et al.* Age of first exposure to football and later-life cognitive impairment in former NFL players. *Neurology* **84**, 1114–1120 (2015).
30. Kuzminski, S. J. *et al.* White Matter Changes Related to Subconcussive Impact Frequency during a Single

Season of High School Football. *AJNR Am. J. Neuroradiol.* **39**, 245–251 (2018).

31. Montenigro, P. H. *et al.* Cumulative Head Impact Exposure Predicts Later-Life Depression, Apathy, Executive Dysfunction, and Cognitive Impairment in Former High School and College Football Players. *J. Neurotrauma* **34**, 328–340 (2017).
32. Lemon, R. N. & Griffiths, J. Comparing the function of the corticospinal system in different species: Organizational differences for motor specialization? *Muscle Nerve* **32**, 261–279 (2005).
33. Wu, Y.-C. *et al.* Hybrid Diffusion Imaging in Mild Traumatic Brain Injury. *J. Neurotrauma* **35**, 2377–2390 (2018).
34. Lebel, C. *et al.* Diffusion tensor imaging of white matter tract evolution over the lifespan. *NeuroImage* **60**, 340–352 (2012).
35. Bahrami, N. *et al.* Subconcussive Head Impact Exposure and White Matter Tract Changes over a Single Season of Youth Football. *Radiology* **281**, 919–926 (2016).
36. Champagne, A. A., Coverdale, N. S., Germuska, M. & Cook, D. J. Multi-parametric analysis reveals metabolic and vascular effects driving differences in BOLD-based cerebrovascular reactivity associated with a history of sport concussion. *Brain Inj.* **33**, 1479–1489 (2019).
37. Eyolfson, E., Khan, A., Mychasiuk, R. & Lohman, A. W. Microglia dynamics in adolescent traumatic brain injury. *J. Neuroinflammation* **17**, 326 (2020).
38. Aungst, S. L., Kabadi, S. V., Thompson, S. M., Stoica, B. A. & Faden, A. I. Repeated Mild Traumatic Brain Injury Causes Chronic Neuroinflammation, Changes in Hippocampal Synaptic Plasticity, and Associated Cognitive Deficits. *J. Cereb. Blood Flow Metab.* **34**, 1223–1232 (2014).
39. Clark, C. M. *et al.* Effect of aerobic exercise on white matter microstructure in the aging brain. *Behav. Brain Res.* **373**, 112042 (2019).
40. Haeger, A., Costa, A. S., Schulz, J. B. & Reetz, K. Cerebral changes improved

by physical activity during cognitive decline: A systematic review on MRI studies. *NeuroImage Clin.* **23**, 101933 (2019).

41. Slobounov, S. M. *et al.* The effect of repetitive subconcussive collisions on brain integrity in collegiate football players over a single football season: A multi-modal neuroimaging study. *NeuroImage Clin.* **14**, 708–718 (2017).